Voltage and temperature dependencies of conductivity in gated graphene

F.T. Vasko[1,2*] and V. Ryzhii[2,3]
[1] *Institute of Semiconductor Physics, NAS of Ukraine, Pr. Nauki 41, Kiev, 03028, Ukraine*
[2] *University of Aizu, Ikki-machi, Aizu-Wakamatsu 965-8580, Japan*
[3] *Japan Science and Technology Agency, CREST, Tokyo 107-0075, Japan*
(Dated: February 1, 2008)

The resistivity of gated graphene is studied taking into account electron and hole scattering by short- and long-range structural imperfections (the characteristics of disorder were taken from the scanning tunneling microscopy data) and by acoustic phonons. The calculations are based on the quasiclassical kinetic equation with the normalization condition fixed by surface charge. The gate-voltage and temperature effects on the resistance peak, which is centered at the point of intrinsic conductivity, are found to be in agreement with the transport measurements.

PACS numbers: 72.10.-d, 73.63.-b, 81.05.Uw

Numerous features of electronic properties of graphene (see discussion and Refs. in 1 and 2) are caused by both a neutrino-like dynamics of carriers [3], which is described by the Weyl-Wallace model [4], and a substantial modification of scattering processes. For instance, the gapless energy spectrum and specific character of scattering are responsible for the peak of resistance of the gated graphene sheet (Fig. 1a). Such a peak was observed in Refs. 1 and 5-9 and one appears due to the transformation between n- and p-types of conductivity through the intrinsic region with the chemical potential in the vicinity of the band cross-point. Moreover anomalous temperature dependence was found: the peak resistance decreases with temperature while the tail resistance increases. To the best of our knowledge, a qualitative description of the gate-voltage and temperature effects on conductivity is not performed yet. Much attention was attached to the minimal conductivity phenomena, see last papers, [10] and the metallic regime of conductivity was also examined. [11] Recently, the near-maximum shape of the graphene resistance was considered assuming the scattering by a remote charge impurities layer is a dominant scattering mechanism. [9] Since the high-density layer is not likely to be present, an additional scattering due to disorder was suggested in Ref. 12, but the only metallic regime of conductivity was discussed.

In this Brief Report, we calculate the gate-voltage and temperature dependencies of the resistivity peak taking into account structural inhomogeneities of graphehe [both long-range inhomogeneities and point defects, Figs. 1b and 1c, respectively] and the acoustic phonon scattering. Our model is justified by the recent scanning tunneling microscopy (STM) measurements, [13] where both the imperfections with the lateral scale of 5−9 nm and point defects were reported. The long-range disorder (DL) is described by the potential $U_{\mathbf{x}}$ with the Gaussian correlation function $\langle U_{\mathbf{x}}U_{\mathbf{x}'}\rangle \equiv \overline{U_l}^2 \exp\{-[(\mathbf{x}-\mathbf{x}')/l_c]^2\}$ where $\overline{U_l}$ is the averaged energy and l_c is the correlation length. The short-range defects (DS) of sheet density n_d are approximated by the potential $U_d\Delta(\mathbf{x})$ where $\Delta(\mathbf{x})$ is a function localized over the scale l_d^2. The main contribution to the acoustic phonon scattering appears due to the deformation interaction with longitudinal vibrations, [14, 15] $D\nabla\cdot\mathbf{u}_{\mathbf{x}}$, where D is the deformation potential and $\mathbf{u}_{\mathbf{x}}$ is the displacement vector of LA-mode.

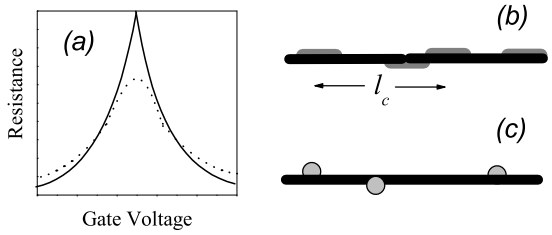

FIG. 1: (a) Schematic plot of the resistance at zero (solid) and finite (dotted) temperatures versus gate voltage. Nonideal sheet of graphene (b) with a long-range inhomogeneities (gray) and (c) with point defects marked by balls.

The peak of resistance is originated from the distinctions of scattering caused by DS (or LA) and DL mechanisms. Since a short-range relaxation rate (due to DS contribution or LA phonon scattering at high temperatures) is proportional to the density of states [11], the resistance R does not change with concentration or gate voltage V_g. Besides, the LA contribution is proportional to temperature of phonons T, and R increases with T. In contrast, the DL scattering becomes suppressed if an electron (hole) momentum exceeds $\hbar/l_c$. Due to this, R decreases when V_g or T (i.e. energy of carriers) increases. Thus, a combination of DL- and DS- (LA-) mechanisms allows an explanation of an experimental behaviour shown in Fig.1a.

Scattering between electron or hole states [16] with two-dimensional momenta $\mathbf{p}$ and $\mathbf{p}'$ is described by the transition probabilities $W^{ß(j)}_{\mathbf{p},\mathbf{p}'}$ where $j = DL$, DS, and LA. Within the Born approximation, $W^{ß(j)}_{\mathbf{p},\mathbf{p}'}$ is written in

*Electronic address: ftvasko@yahoo.com

the golden rule form,

$$W^{ß(j)}_{\mathbf{p},\mathbf{p}'} = \frac{2\pi}{\hbar} W^{ß(j)}_q \Psi_\theta \delta[v_{ßW}(p-p')], \tag{1}$$

where the overlap factor $\Psi_\theta = (1+\cos\theta)/2$ with $\theta = \widehat{\mathbf{p}',\mathbf{p}}$ describes the suppression of backscattering processes, [17] $v_{ßW} \simeq 10^8$ cm/s is the characteristic velocity of the linear dispersion laws, $\pm v_{ßW} p$, with the upper and lower signs corresponding to electrons and holes, respectively. The matrix element $W^{ß(j)}_q$, which depends on the momentum transfer $\hbar\mathbf{q} = \mathbf{p} - \mathbf{p}'$, is given by

$$W^{ß(j)}_q = \begin{cases} \overline{U}_l^2 \pi l_c^2 e^{-(ql_c/2)^2} & (DL) \\ n_d U_d^2 \pi^2 l_d^4 & (DS) \\ |C_q|^2 2T/\hbar\omega_q & (LA). \end{cases} \tag{2}$$

Here the DL and DS mechanisms of scattering by static disorder are described by the Fourier transformations of $\langle U_{\mathbf{x}} U_{\mathbf{x}'}\rangle$ and $U_d\Delta(\mathbf{x})$. The LA probability is expressed via the matrix element $|C_q|^2 = D^2\hbar\omega_q/(2\rho_s s^2 L^2)$, where s is the sound velocity, $\omega_q = sq$ is the phonon frequency, ρ_s is the sheet density of graphene, and L^2 is the normalization area. Within the equipartition condition, at $\hbar\omega_q \ll T$, we replace the Planck distribution of phonons by $T/\hbar\omega_q$.

Under the steady-state electric field, $\mathbf{E}$, the electron (e) and hole (h) distribution functions, $f_{e\mathbf{p}}$ and $f_{h\mathbf{p}}$, are governed by the quasiclassical kinetic equations (here and below $k = e, h$),

$$e\mathbf{E}\cdot\frac{\partial f_{k\mathbf{p}}}{\partial \mathbf{p}} = \sum_{j\mathbf{p}'} W^{ß(j)}_{\mathbf{p},\mathbf{p}'}(f_{k\mathbf{p}'} - f_{k\mathbf{p}}), \tag{3}$$

with the standard collision integral for the elastic scattering. [18] Using the electron and hole velocities $\pm v_{ßW}\mathbf{p}/p$, one obtains the following expression for the current density:

$$\mathbf{I} = \frac{4ev_{ßW}}{L^2}\sum_{\mathbf{p}}\frac{\mathbf{p}}{p}\left(f_{e\mathbf{p}} + f_{h\mathbf{p}}\right), \tag{4}$$

where factor 4 appears due to the spin and valley degeneracy. The distribution functions $f_{e\mathbf{p}}$ and $f_{h\mathbf{p}}$ are also related to each other and to the sheet charge density, Q_s,

$$Q_s = \frac{4e}{L^2}\sum_{\mathbf{p}}\left(f_{e\mathbf{p}} - f_{h\mathbf{p}}\right). \tag{5}$$

Note, that Q_s can be expressed via the gate voltage as $V_g = \epsilon Q_s/4\pi d$. Below we assume the SiO_2 substrate of the width d =3 nm with the dielectric permittivity $\epsilon \simeq$3.

Within the linear approximation, the solution of Eq. (3) can be seached in the form $f_{k\mathbf{p}} = F_{kp} + \Delta f_{k\mathbf{p}}$, where $F_{kp} = \{\exp[(v_{ßW}p \mp \mu)/T] + 1\}^{-1}$ are the equilibrium Fermi distributions with the chemical potential μ. The asymmetric parts of distribution functions, $\Delta f_{k\mathbf{p}}$, can be obtained from Eq. (3) in the form

$$\Delta f_{k\mathbf{p}} = -\frac{(e\mathbf{E}\cdot\mathbf{p})}{p}\tau_p^{ß(m)}\left(-\frac{dF_{kp}}{dp}\right), \tag{6}$$

with the momentum relaxation time, $\tau_p^{ß(m)}$, is given by the sum of relaxation rates $\tau_p^{ß(m)} = \left[\sum_j (1/\tau_p^{ß(j)})\right]^{-1}$ where $1/\tau_p^{ß(j)} = \sum_{\mathbf{p}'} W^{ß(j)}_{\mathbf{p},\mathbf{p}'}(1-\cos\theta)$. Substituting Eq. (6) into Eq. (4) one obtains the resistivity, which is introduced by $\mathbf{I} = \mathbf{E}/R$, as follows:

$$\frac{1}{R} = \frac{e^2 v_{ßW}}{\pi\hbar^2}\int_0^\infty dp\; p\tau_p^{ß(m)}\sum_k\left(-\frac{dF_{kp}}{dp}\right) \tag{7}$$

and the momentum relaxation time here do not depend on k. It is convenient to present the relaxation rates as

$$\frac{1}{\tau_p^{ß(j)}} = \frac{v_{sc}^{ß(j)} p}{\hbar}\begin{cases}\Psi\left(pl_c/\hbar\right) & (DL) \\ 1 & (DS,\ LA),\end{cases} \tag{8}$$

where the averaging over angle gives the function

$$\Psi(z) = \frac{e^{-z^2/2}}{z^2} I_1\left(\frac{z^2}{2}\right), \tag{9}$$

with the first-order Bessel function of an imaginary argument, $I_1(x)$. The characteristic velocities, $v_{sc}^{ß(j)}$, in Eq. (8) are introduced as follows:

$$v_{sc}^{ß(j)} = \frac{1}{4\hbar^2 v_{ßW}}\begin{cases}\pi\overline{U}_l^2 l_c^2 & (DL) \\ \pi^2 U_d^2 l_d^3 n_d & (DS) \\ D^2 T/(\rho_s s^2) & (LA),\end{cases} \tag{10}$$

so that $v_{sc}^{ß(j)} \ll v_{ßW}$ for the parameters used below.

Next, we simplify the expression (7) using the dimensionless resistivity, $Re^2/\pi\hbar$. We consider the case of degenerate carriers, $|\mu| \gg T$, when Eq. (5) gives the square-root dependence of μ on the gate-voltage: $\mu = \hbar v_{ßW}\sqrt{\epsilon V_g/4|e|d}$. Since $\sum_k(-dF_{kp}/dp)$ can be replaced by δ-function, Eqs. (7)-(9) yield the dimensionless resistivity in the following form:

$$R\frac{e^2}{\pi\hbar} = \frac{v_{sc}^{ß(DL)}}{v_{ßW}}\Psi\left(\frac{\mu l_c}{v_{ßW}\hbar}\right) + \frac{v_{sc}^{ß(DS)}}{v_{ßW}} + \frac{v_{sc}^{ß(LA)}}{v_{ßW}}, \tag{11}$$

with the temperature dependent LA contribution $v_{sc}^{ß(LA)}/v_{ßW}$. Another simple expression can be obtained for the case of the intrinsic regime of transport, $Q_s = 0$, when μ=0 and $F_{kp} \to [\exp(v_{ßW}p/T)+1]^{-1}$ in Eq.(7). As a result, the inverse sheet resistance is expressed through the dimensionless integral,

$$\frac{\pi\hbar}{Re^2} = \frac{v_{sc}^{ß(DL)}}{v_{ßW}}\int_0^\infty \frac{dx}{1+\cosh x} \times\left[\Psi\left(x\frac{Tl_c}{v_{ßW}\hbar}\right) + \frac{v_{sc}^{ß(DS)}}{v_{ßW}} + \frac{v_{sc}^{ß(LA)}}{v_{ßW}}\right]^{-1}. \tag{12}$$

Here, not only the ratio $v_{sc}^{ß(LA)}/v_{ßW}$ increases with the temperature but also the DL contribution becomes suppressed, if $Tl_c/v_{ßW}\hbar > 1$.

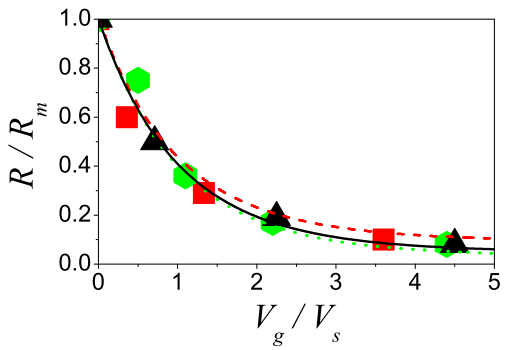

FIG. 2: (Color online) Normalized resistance R/R_m versus dimensionless gate voltage V_g/V_s plotted for parameters of ref. 1 (dotted curve, hexagons), Ref. 7 (solid curve, triangles) and Ref. 8 (dashed curve, squares).

We turn now to discussion of the experimental data using the parameters of Eq. (2) in order to fit the gate-voltage and temperature dependencies of resistance obtained in Refs. 1, 7, and 8 (similar low-temperature results can be obtained from Refs. 6 and 9). Under the description of the LA scattering we use the known parameters $s \simeq 7.3 \cdot 10^5$ cm/s and $\rho_s \simeq 7 \cdot 10^{-8}$ g/cm^2. In order to obtain the temperature-dependent contribution to the tails of peak [about 100 Ω in Fig.2a of Ref. 7 and in Fig.1 of Ref.8] one needs the deformation potential $D \simeq$12 eV which is about 75% of the graphite value. [14, 17] For such a set of parameters, one obtains $v_{sc}^{ß(LA)} \simeq 8 \cdot 10^5$ cm/s at T=300 K from Eq. (11). Since $\Psi(z \to \infty) = 0$, the temperature independent part of the tails, which is about 400 Ω in Fig. 1 of Refs. 1 and 8 and about 200 Ω in Fig. 2a of Ref. 7, appears due to the DS contribution with the characteristic velocities $v_{sc}^{ß(DS)} \simeq 3.2 \cdot 10^6$cm/s and $1.6 \cdot 10^6$cm/s for Refs. 1 and 8 and Ref. 7, respectively.

In order to fit the gate-bias dependencies, in Fig. 2 we plot the normalized resistance R/R_m versus the dimensionless gate-bias, V_g/V_s, where $R_m = \pi\hbar(v_{sc}^{ß(DL)} + v_{sc}^{ß(DS)})/v_{ßW}e^2$ and $V_s = 4|e|d/\epsilon l_c^2$. Here we used the values of $v_{sc}^{ß(DS)}$ obtained above and the 5 nm correlation length, which is taken from the STM measurements [13], for all the cases. [1, 7, 8] A good agreement is obtained for $v_{sc}^{ß(DL)} \simeq 3.2 \cdot 10^7$cm/s (Refs. 7 and 8) and $5 \cdot 10^7$cm/s. [1] Thus, we have found the scattering parameters of the relaxation rates given by Eqs. (8) and (9) for three different samples and one can plot $\nu_p^{ß(j)}$ versus energy $v_{ßW}p$ (see Fig. 3). The velocities $\nu_p^{ß(DL,DS)}$ are connected to the characteristic potentials $\overline{U}_l$ and U_d as follows. For the long-range disorder, we obtain $\overline{U}_l \sim$100 meV or 80 meV for Ref. 1 or Refs. 7 and 8, respectively, i.e. $\overline{U}_l$ is less than the interlayer coupling energy ∼350 meV. The energy U_d can be estimated as ∼3 eV (of the order of the intralayer coupling energy), if we use $l_d \simeq$2

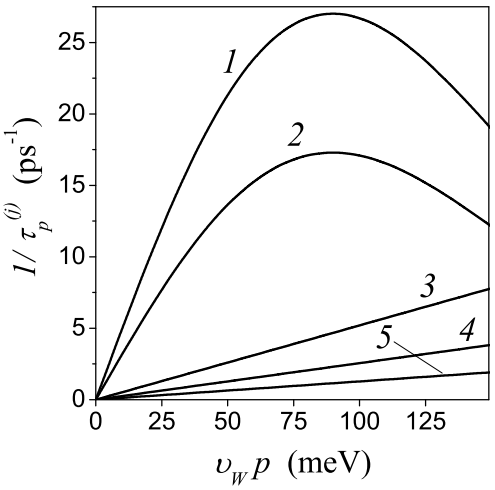

FIG. 3: Relaxation rates $1/\tau_p^{ß(j)}$ versus energy, $v_{ßW}p$: (1) $j = DL$ for parameters of Refs. 7 and 8, (2) $j = DL$ for Ref.1, (3) $j = DS$ for Refs. 1 and 7, (4) $j = DS$ for Ref. 8, and (5) $j = LA$ for Refs. 1, 7, and 8.

nm and $n_d l_d^2 \sim 1\%$. The suppression of resistance with V_g takes place if the chemical potential exceeds the 100 meV threshold, see Fig. 3 ($\mu \sim$50 meV at V_g=10 V for the structures under consideration). Thus, both voltage-induced and temperature-induced (below 700−1000 K where the optical phonon contribution becomes essential) suppression of resistance takes place.

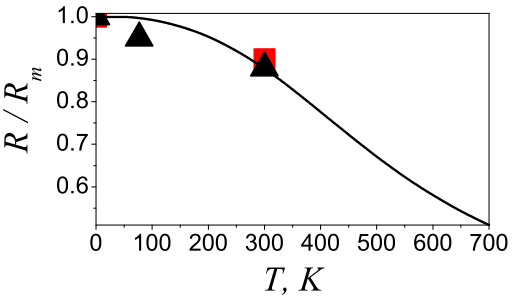

FIG. 4: (Color online) Temperature dependence of resistance R/R_m for the intrinsic regime of conductivity, $\mu = 0$. The experimental data taken from Refs. 7 and 8 are marked as in Fig. 2.

Due to lack of data on the temperature dependency of resistance, we only discuss here the suppression of the resistance peak value when temperature increases. We use Eq. (12) which governs the intrinsic regime of conductivity and the dependency $R(T)$ is in agreement with the room temperature data of Refs. 7 and 8 without any additional parameters. Figure 4 shows an essential suppression of R when the ratio $Tl_c/v_{ßW}\hbar$ exceeds unit (at $T >$300 K for the parameters used). An extrapolation for the high-temperature region shows an essential

suppression of the DL scattering at $T \geq$1000 K. Thus, a minimum of resistance, which is caused by such a suppression and an optical phonon contribution, should take place for the temperature region above $\sim$ 500 K.

Let us discuss the approximations used in our calculations. The main assumption of our model is the phenomenological description of the elastic scattering by long- and short-range structural inhomogeneities. While the in-plane scales of disorder, l_c and l_d, are clear and justified by Ref. 13, a nature of inhomogeneities and a value of the phenomenological energies [$\overline{U}_l$ and U_d in Eq.(2)] require an additional analysis. Other approximations made are rather standard and generally accepted. We have neglected the screening effects because it is not a leading effect for a spatial ranges up to 5 nm. The only scattering by LA mode is taken into account because another contributions are weaker (see Refs. 14 and 17 and references therein). Since $v_{sc}^{ß(j)} \ll v_{ßW}$, the (anti)localization phenomena [19] can be neglected if $Re^2/\pi\hbar \ll 1$ (but it may be essential in Ref. 5 and in Fig. 3 of of Ref. 7, where $R_m \sim 10$ KΩ). In addition, the quantum dynamics restrictions, like a Zitterbewegung effect [20] or the field-induced interband tunneling, are only essential in the vicinity of the cross-point. Since R is weakly changed near this point, one can use the results obtained as phenomenological dependencies. However, a justification for the scales $\sim$1 V or tens of kelvins is beyond of the consideration performed.

In summary, we have found that the main factor, which forms the resistance peak centered at the intrinsic conductivity region, is a structure disorder (e.g., defect clusters, bilayer islands, or a substrate disorder [21]) with the scale around 5 nm for the samples analyzed. Short-range defect contribution and acoustic phonon scattering are only essential for the heavily doped case on the tails of peak. Both gate-voltage and temperature-induced quenchings of the resistance peak are in agreement with the transport measurements [1, 7, 8] and with the STM mapping of nonideal graphene sheet. [13] A complete verification of the mechanism suggested requires both microscopic calculations (in order to estimate the fitting parameters $\overline{U_l}$ and U_d) and a further investigation of the transport phenomena. Particularly, high-temperature conductivity measurements, which can confirm a suppression of resistance peak, as well as treatment of magnetotransport and high-frequency responses are necessary.

To conclude, the results presented permit to analyze linear characteristics of the graphene-based field-effect transistor. Recent studies of such a device, see Ref. 22 and references therein, demonstrated an essential gate modulation. However, the data available are not sufficient to determine the scattering mechanisms. We believe that t result obtained will stimulate further investigations in order to understand transport phenomena and to improve device characteristics.

The work at the University of Aizu was partially supported by the Grant-in-Aid for Scientific Research (S) from the Japan Society for Promotion of Science and by the Japan Science and Technology Agency, CREST.

[1] A.K. Geim and K.S. Novoselov, Nature Materials **6**, 183 (2007).

[2] M.I. Katsnelson, K.S. Novoselov, A.K. Geim. Nature Phys. **2** 620 (2006); M.I. Katsnelson, Materials Today **10**, 20 (2007).

[3] E.M. Lifshitz, L.P. Pitaevskii, and V.B. Berestetskii, Quantum Electrodynamics, (Butterworth-Heinemann, Oxford 1982).

[4] H. Weyl, *The Theory of Groups and Quantum Mechanics*, (Dover, N.Y.1950); P.R. Wallace, Phys. Rev. **71**, 622 (1947).

[5] K.S. Novoselov, A.K. Geim, S.V. Morozov, D. Jiang, Y. Zhang, S.V. Dubonos, I.V. Grigorieva, A.A. Firsov, Science, **306** 366 (2004).

[6] Y. Zhang, Y.-W. Tan, H.L. Stormer, and P. Kim, Nature **10**, 201 (2005).

[7] Y.-W. Tan, Y. Zhang, H.L. Stormer, and P. Kim, Eur. Phys. J. Special Topics **148**, 15 (2007).

[8] E.W. Hill, A.K. Geim, K. Novoselov, F. Schedin and P. Blake, IEEE Trans. Magn. **42**, 2694 (2006); see also arXiv0704.3165.

[9] Y. -W. Tan, Y. Zhang, K. Bolotin, Y. Zhao, S. Adam, E. H. Hwang, S. Das Sarma, H. L. Stormer, P. Kim, arXiv:0707.1807; E.H. Hwang, S. Adam, and S. Das Sarma, Phys. Rev. Lett. **98**, 186806 (2007).

[10] P.M. Ostrovsky, I.V. Gornyi, and A.D. Mirlin, Phys. Rev. B **74**, 235443 (2006); K. Nomura and A.H. MacDonald, Phys. Rev. Lett. **98**, 076602 (2007); K. Ziegler Phys. Rev. B 75, 233407 (2007).

[11] T. Ando, J. Phys. Soc. Japan, **75**, 074716 (2006); L.A. Falkovsky, Phys. Rev. B **75** 033409 (2007); M.I. Katsnelson and A.K. Geim, arXiv:0706.2490.

[12] T. Stauber, N.M.R. Peres, and F. Guinea, arXiv:0707.3004; N.M.R. Peres, J.M.B. Lopes dos Santos, and T. Stauber, Phys. Rev. B **76**, 073412 (2007).

[13] G. M. Rutter, J.N. Crain, N.P. Guisinger, T. Li, P.N. First, J.A. Stroscio, Science **317**, 219 (2007); E. Stolyarova, K.T. Rim, S. Ryu, J. Maultzsch, P. Kim, L.E. Brus, T.F. Heinz, M.S. Hybertsen, and G.W. Flynn, PNAS **104**, 9209 (2007).

[14] H. Suzuura and T. Ando, Phys. Rev. B **65**, 235412 (2002).

[15] L. M. Woods and G. D. Mahan, Phys. Rev. B **61**, 10651 (2000).

[16] The interband transitions are forbidden both for static disorder (due to energy conservation) and for LA-mode (due to the condition $s < v_{ßW}$).

[17] R. Saito, G. Dresselhaus, M. S. Dresselhaus, *Physical Properties of Carbon Nanotubes*, Imperial College Press, London, UK (1999).

[18] J.M. Ziman, *Electrons and Phonons* (Qxford University Press, Qxford 2001); F.T. Vasko and O.E. Raichev,

Quantum Kinetic Theory and Applications (Springer, N.Y. 2005).

[19] S.V. Morozov, K.S. Novoselov, M.I. Katsnelson, F. Schedin, L.A. Ponomarenko, D. Jiang, and A.K. Geim, Phys. Rev. Lett. **97**, 016801 (2006); E. McCann, K. Kechedzhi, V.I. Fal'ko, H. Suzuura, T. Ando, and B.L. Altshuler, Phys. Rev. Lett. **97**, 146805 (2006); A.F. Morpurgo and F. Guinea, Phys. Rev. Lett. **97**, 196804 (2006).

[20] W. Zawadzki, Phys. Rev. B **72**, 085217 (2005); M. Auslender and M. I. Katsnelson, arXiv:0707.2804.

[21] M. Ishigami, J.H. Chen, W.G. Cullen, M.S. Fuhrer, and E.D. Williams, Nano Letters **7** 1643 (2007).

[22] M.C. Lemme, T.J. Echtermeyer, M. Baus, and H. Kurz, IEEE Electron Device Lett. **28** 282 (2007).